LETTER

Enhancement of Ohmic heating by Hall current in magnetized capacitively coupled discharges

To cite this article: Bocong Zheng *et al* 2019 *Plasma Sources Sci. Technol.* **28** 09LT03

Letters

IOP Publishing — Plasma Sources Science and Technology

Plasma Sources Sci. Technol. **28** (2019) 09LT03 (5pp) https://doi.org/10.1088/1361-6595/ab419d

Letter

Enhancement of Ohmic heating by Hall current in magnetized capacitively coupled discharges

Bocong Zheng[1], **Keliang Wang**[1], **Timothy Grotjohn**[1,2], **Thomas Schuelke**[1,2] **and Qi Hua Fan**[1,2,3,4]

[1] Fraunhofer Center for Coatings and Diamond Technologies, Michigan State University, East Lansing, MI 48824, United States of America
[2] Department of Electrical and Computer Engineering, Michigan State University, East Lansing, MI 48824, United States of America
[3] Department of Chemical Engineering and Materials Science, Michigan State University, East Lansing, MI 48824, United States of America

E-mail: qfan@egr.msu.edu

Received 19 July 2019, revised 19 August 2019
Accepted for publication 5 September 2019
Published 24 September 2019

Abstract

In low-pressure capacitively coupled discharges, a heating mode transition from a pressure-heating dominated state to an Ohmic-heating dominated state is known by applying a small transverse magnetic field. Here we demonstrate via particle-in-cell simulations and a moment analysis of the Boltzmann equation that the enhancement of Ohmic heating is induced by the Hall current in the $\boldsymbol{E} \times \boldsymbol{B}$ direction. As the magnetic field increases, the Ohmic heating in the $\boldsymbol{E} \times \boldsymbol{B}$ direction dominates the total electron power absorption. The Ohmic heating induced by the Hall current can be well approximated from the Ohmic heating of unmagnetized capacitively coupled discharges.

Supplementary material for this article is available online

Keywords: capacitively coupled plasmas, electron power absorption, magnetic field, moments of Boltzmann equation, particle in cell simulations, Ohmic heating

Capacitively coupled discharges are widely used for modern plasma processing applications. One of the most important issues of capacitively coupled plasmas (CCPs) is the mechanism of electron power absorption from radio-frequency (rf) fields, also called 'electron heating'. At high pressures, Ohmic heating due to electron collisions with neutrals plays a primary role. At low pressures, an additional 'collisionless' (also referred to as stochastic) heating mechanism is required to sustain the discharge [1]. According to the widely accepted hard wall model [2], this 'collisionless' electron power absorption is from the momentum transfer of electrons with the oscillating sheath. Another explanation is the pressure heating due to the electron pressure gradient [3, 4], which stems from the same basic physical mechanism as the hard wall model [5]. The presence of a transverse magnetic field can appreciably inhibit the motion of electrons along the electric field. Turner *et al* [6] demonstrated a heating mode transition from pressure heating to Ohmic heating by applying a small transverse magnetic field of about 10 G. Later, the discharge characteristics of magnetized CCPs were investigated experimentally [7–9] and numerically [10, 11]. However, so far, the existed models can only explain part of the heating mechanisms, there has been no self-consistent and complete investigation of electron heating in magnetized CCPs.

In this work, we make use of a moment analysis of the Boltzmann equation [12–14] to investigate the electron heating in magnetized CCPs for the first time. This analysis

[4] Author to whom correspondence should be addressed.

does not use any ad hoc assumptions and therefore includes all electron power absorption mechanisms. The magnetized Boltzmann equation for electrons is

$$\frac{\partial f_e}{\partial t} + \boldsymbol{v}\cdot\ \nabla f_e - \frac{e}{m_e}(\boldsymbol{E} + \boldsymbol{v} \times \boldsymbol{B}) \cdot \nabla_v f_e = \left.\frac{\partial f_e}{\partial t}\right|_c, \quad (1)$$

where f_e is the electron distribution function, $\boldsymbol{v}$ the velocity, m_e and e the electron mass and charge, t the time, $\boldsymbol{E}$ and $\boldsymbol{B}$ the electric and magnetic fields. Multiplying the Boltzmann equation by $\boldsymbol{v}$ and integrating all terms of (1) over velocity space, we obtain the momentum conservation equation for electrons

$$\begin{aligned} m_e n_e \frac{\partial \boldsymbol{u}_e}{\partial t} + m_e(\boldsymbol{\Gamma}_e\cdot\ \nabla)\boldsymbol{u}_e &= -en_e(\boldsymbol{E} + \boldsymbol{u}_e \times \boldsymbol{B}) \\ &\quad - \nabla\cdot\ \overleftrightarrow{\boldsymbol{\Pi}}_e + \left(\frac{\partial \rho_e}{\partial t}\right)_c \end{aligned}, \quad (2)$$

where n_e, $\boldsymbol{u}_e$, $\boldsymbol{\Gamma}_e$, $\overleftrightarrow{\boldsymbol{\Pi}}_e$ and $(\partial\rho_e/\partial t)_c$ are the electron density, drift velocity, drift flux, pressure tensor and change of momentum due to collisions, respectively (see supplementary materials for detailed definitions is available online at stacks.iop.org/PSST/28/09LT03/mmedia). In one-dimension, assuming an electric field in the x-direction and a transverse magnetic field in the y-direction, the total power absorption by electrons per unit volume is given by $P_{abs} = \boldsymbol{J}\cdot\boldsymbol{E} = J_{e,x}E_x$, where $\boldsymbol{E} = (E_x, E_y, E_z) = (E_x, 0, 0)$ and $J_{e,x} = -en_e u_{e,x}$ is the electron current density in the x-direction. It should be noted that there are strong Hall fields, $E_{H,x} = -u_{e,z}B_y$ in the x-direction and $E_{H,z} = u_{e,x}B_y$ in the z-direction. However, the forces generated by the Hall fields do not contribute to the electron heating. Multiplying each component of equation (2) in different directions with the corresponding drift velocities, we obtain the electron mechanical energy conservation equations in the x-, y-and z-directions. The contribution of Hall fields in these equations are eliminated since $u_{e,x}E_{H,x} + u_{e,z}E_{H,z} = 0$. The sum of these equations gives the total electron mechanical energy conservation equation

$$P_{abs} = P_{in} + P_{press} + P_{Ohmic}, \quad (3)$$

where

$$\begin{aligned} P_{in} &= m_e n_e \sum_i u_{e,i}\frac{\partial u_{e,i}}{\partial t} + m_e \sum_i u_{e,i}\Gamma_{e,x}\frac{\partial u_{e,i}}{\partial x}, \\ P_{press} &= \sum_i u_{e,i}\frac{\partial \Pi_{e,xi}}{\partial x}, \\ P_{Ohmic} &= -\sum_i u_{e,i}\left(\frac{\partial \rho_{e,i}}{\partial t}\right)_c, \end{aligned} \quad (4)$$

are the electron heating from the inertial terms, the pressure heating component and the Ohmic heating component, $i = x, y, z$ is the axis coordinate.

We use a custom developed code, ASTRA, which based on the electrostatic implicit particle-in-cell algorithm with Monte Carlo collisions (PIC/MCC), for all the simulations described here. The simulation is in one-dimension, with an electrode separation of $L = 5$ cm. A rf source with a voltage amplitude of 150 V and a frequency of 15 MHz is connected to the left electrode, the right electrode is grounded. To simplify the analysis, the external circuit, secondary electron emission and electron reflection are not considered. The neutral gas is argon, uniformly distributed in space with a temperature of 300 K and a pressure of 10 mTorr. The cross sections of charged particles with neutrals are taken from [15]. The description of the ASTRA code, the benchmark with [16], as well as the details of simulations can be found in the supplementary materials.

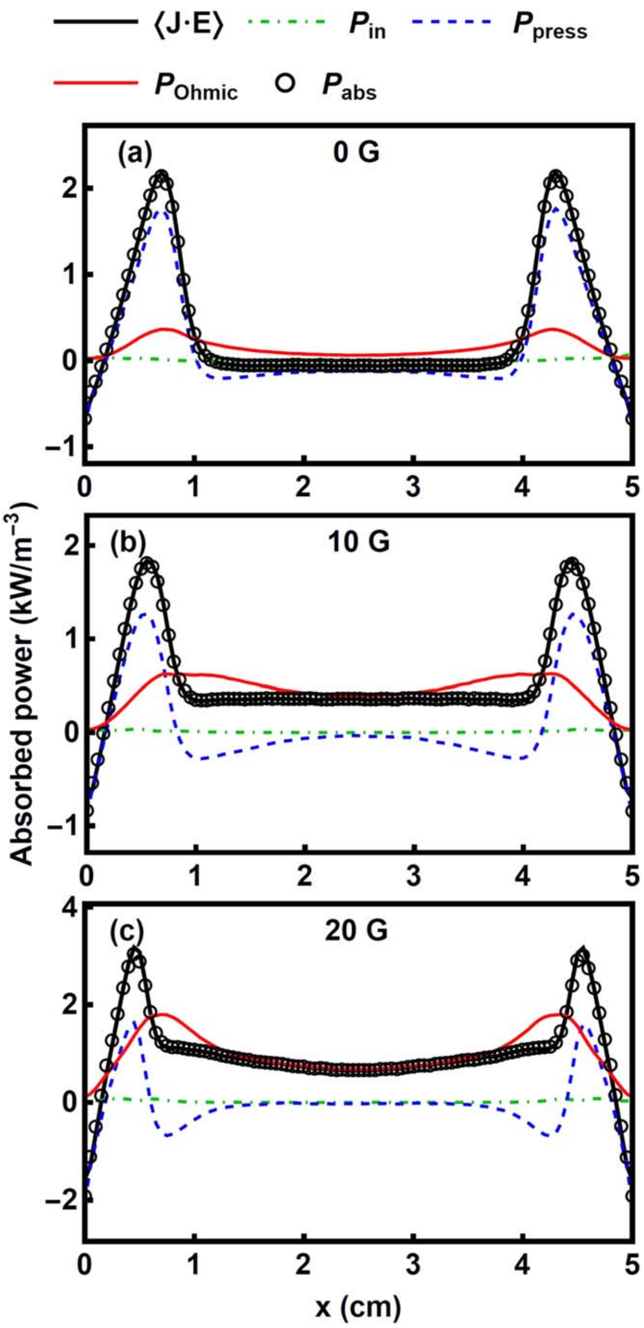

Figure 1. Spatial profiles of time-averaged electron power absorption for transverse magnetic fields of 0, 10, and 20 G. The electrode separation is 50 mm and the pressure is 10 mTorr.

Figure 1 shows the spatial profiles of time-averaged power absorption for various transverse magnetic fields. In all cases the power absorption P_{abs} from the sum of each heating

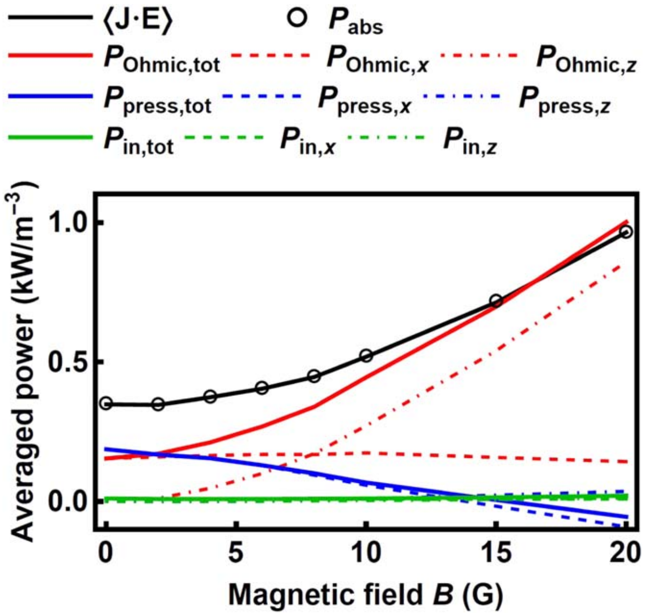

Figure 2. Electron heating components as a function of transverse magnetic field.

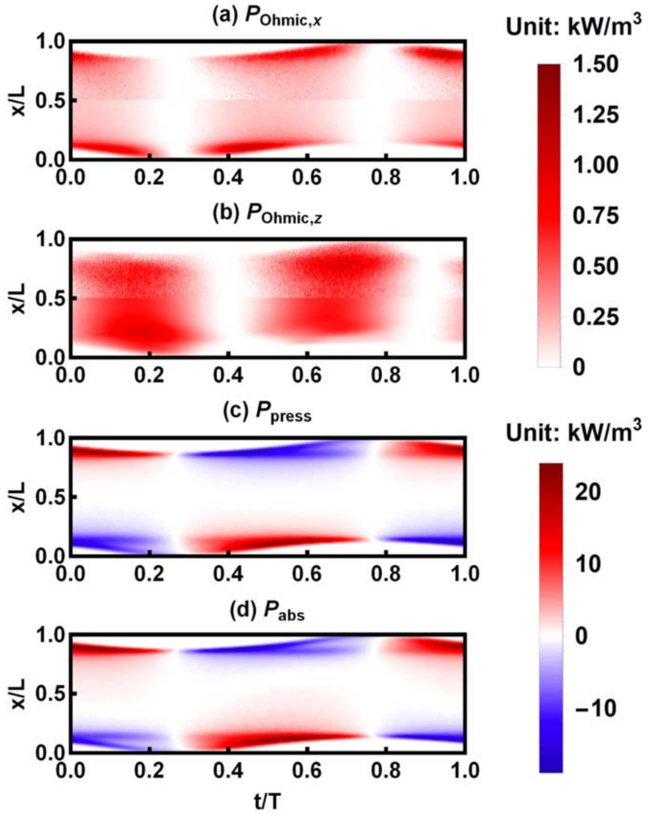

Figure 3. Space- and time-resolved electron power absorptions during one RF period at 10 G.

component matches well with the power absorption directly calculated from $\langle \boldsymbol{J} \cdot \boldsymbol{E} \rangle$. The contribution from inertial terms can be neglected for all magnetic fields, similar to the case of unmagnetized CCPs [13, 14]. Without the magnetic field, the heating peaks in the sheath region and approaches zero in the bulk region. As the magnetic field increases, a net heating in the bulk region appears. These phenomena have previously been observed [17] and attributed to a reduction in the effective mean free path of the electrons. Now, by decomposing the electron heating into different components, we confirm that the bulk heating in magnetized CCPs is mainly contributed by the Ohmic heating.

Figure 2 demonstrates the variations of each heating component as a function of the magnetic field, the heating components are space- and time-averaged. As the magnetic field increases, the Ohmic heating rises and the pressure heating declines, resulting in a heating mode transition, which has been predicted by the pressure heating model under the similar discharge parameters [6]. From equation (4) it can be seen that the electron heating in magnetized discharges can be decomposed into components in different directions, which are also shown figure 2. In one-dimension simulation with an electric field in the x-direction and a transverse magnetic field in the y-direction, only the heating components along the electric field (x-direction) and along the $\boldsymbol{E} \times \boldsymbol{B}$ direction (z-direction) contribute to the electron power absorption, the heating along the magnetic field (y-direction) can be neglected and is not shown. Without the magnetic field the heating components in the $\boldsymbol{E} \times \boldsymbol{B}$ direction are also zero, as shown in figure 2, therefore the heating components in figure 1(a) are equal to the corresponding x-direction components. The spatial profiles of $P_{\text{Ohmic},x}$ at other magnetic fields are all similar to that shown in figure 1(a) (data not shown), and change little with the magnetic fields. The enhancement of Ohmic heating at stronger magnetic fields is a contribution in the z-direction, i.e. the $\boldsymbol{E} \times \boldsymbol{B}$ direction. In addition, as the magnetic field increases, the Ohmic heating in the $\boldsymbol{E} \times \boldsymbol{B}$ direction dominates the total electron power absorption.

The Ohmic heating is induced from the momentum change due to electron-neutral collisions. To understand the enhancement of Ohmic heating in the z-direction, we consider the approximated form of collision term [18, 19]

$$\left(\frac{\partial \rho_{\text{e}}}{\partial t}\right)_c = -m_{\text{e}} \nu_{\text{eff}} n_{\text{e}} u_{\text{e}}, \tag{5}$$

where ν_{eff} is the effective electron momentum transfer collision frequency. The standard approach of using $\nu_{\text{m}} = n_{\text{g}} \int \sigma_{\text{m}} v f_{\text{e}} \mathrm{d}^3 v$ instead of ν_{eff} can significantly underestimate the true collision frequency [20], where n_{g} is the neutral gas density and σ_{m} is the cross-section of electron-neutral momentum transfer collisions. Here we define an effective electron momentum transfer collision frequency $\nu_{\text{eff}} = \frac{\bar{\nu}_{\text{eff}}}{\bar{\nu}_{\text{m}}} \nu_{\text{m}}$, where $\bar{\nu}_{\text{eff}} = \overline{-u_{\text{e}} \left(\frac{\partial \rho_{\text{e}}}{\partial t}\right)_c} \Big/ \overline{m_{\text{e}} n_{\text{e}} u_{\text{e}}^2}$, the overline denote the time and space average. Reconstructing equation (5) yields the standard form of Ohmic heating

$$P_{\text{Ohmic},x} = \frac{m_{\text{e}} \nu_{\text{eff}}}{e^2 n_{\text{e}}} J_{\text{e},x}^2,$$
$$P_{\text{Ohmic},z} = \frac{m_{\text{e}} \nu_{\text{eff}}}{e^2 n_{\text{e}}} J_{\text{e},z}^2. \tag{6}$$

Figure 3 illustrates the space- and time-resolved electron power absorption components during one RF period T at

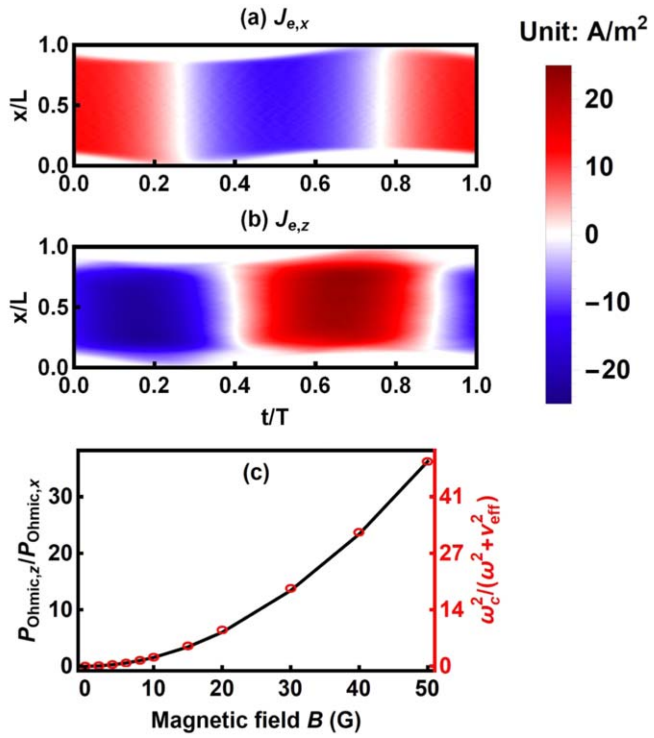

Figure 4. Space- and time-resolved electron conduction currents (a) $J_{e,x}$ and (b) $J_{e,z}$, as well as (c) the ratio of x- to z-direction Ohmic heating and $\omega_{ce}^2/(\omega^2+\nu_{eff}^2)$ as a function of magnetic field.

10 G. The upper part in figures 3(a) and (b), where $x/L = 0.5$–1, is the Ohmic heating calculated directly from the PIC simulation, the lower part of $x/L = 0$–0.5 is calculated from equation (6). The results obtained by different methods show good consistency. The spatio-temporal dynamics of Ohmic heating is well described by equation (6), confirming that the enhancement of Ohmic heating in the z-direction is induced by the Hall current $J_{e,z}$. The Ohmic heating in the bulk region in the z-direction is several times greater than that in the x-direction, due to the Ohmic heating is proportional to J_e, which is stronger in the z-direction (see figure 4 later). The phase shift of Ohmic heating in the x- and z-directions is caused by the currents as well. Figures 3(c) and (d) also gives the space- and time-resolved pressure heating and the sum of all heating components. Although the temporal variation of pressure heating is one order of magnitude higher than the Ohmic heating, the electron cooling during the sheath collapse phase counteracts the heating during the sheath expansion phase, resulting in a lower time-averaged power absorption than the Ohmic heating.

To understand the spatio-temporal behavior of the Ohmic heating, figure 4 gives the space- and time-resolved electron conduction currents at 10 G. The currents $J_{e,x}$ and $J_{e,z}$ are spatially uniform in the bulk region and approximate a sinusoidal change over time. At the midplane of the discharge, the electric field E_x varied sinusoidally with an amplitude of about 0.7 V cm^{-1} (data not shown), the magnetic field B, collision frequency ν_{eff} and electron density n_e are nearly constant, therefore the conduction current at the

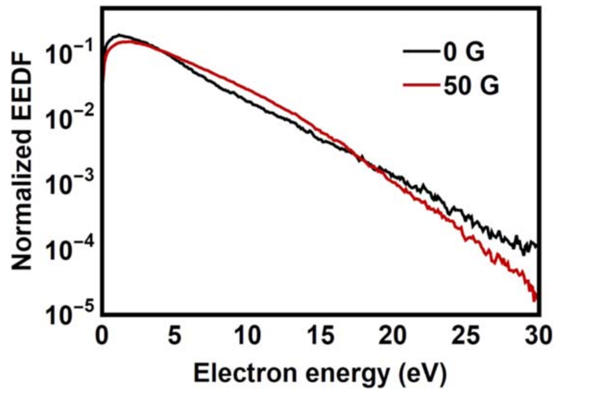

Figure 5. Time-averaged EEDFs at magnetic fields of 0 and 50 G.

midplane can be approximated as [18]

$$J_{e,x} = \kappa_\perp E_x,$$
$$J_{e,z} = -j\kappa_\times E_x, \tag{7}$$

where

$$\kappa_\perp = -\frac{\omega - j\nu_{eff}}{\omega}\frac{\omega_{pe}^2}{(\omega - j\nu_{eff})^2 - \omega_{ce}^2},$$
$$\kappa_\times = \frac{\omega_{ce}}{\omega}\frac{\omega_{pe}^2}{(\omega - j\nu_{eff})^2 - \omega_{ce}^2}, \tag{8}$$

are the plasma dielectric perpendicular to the electric field and along the $\boldsymbol{E} \times \boldsymbol{B}$ direction. In equation (8), ω is the voltage frequency, ω_{pe} the electron plasma frequency, and $\omega_{ce} = eB/m_e$ the electron gyration frequency. The obtained current amplitudes $\tilde{J}_x$ and $\tilde{J}_z$ are about 12 and 23 A m^{-2}, and there is a phase shift of about 0.7π between $J_{e,x}$ and $J_{e,z}$. These results match well with figures 4(a) and (b), and explain the enhanced bulk heating and the phase shift of Ohmic heating in the z-direction. Since the Ohmic heating is approximately proportional to J_e^2, the ratio of x- to z-direction Ohmic heating can be estimated from $|\tilde{J}_z|^2/|\tilde{J}_x|^2$. For the electron mechanical energy conservation in the $\boldsymbol{E} \times \boldsymbol{B}$ direction, the inertial and pressure heating terms can be neglected as shown in figure 2, we have the space- and time-averaged power absorption $\overline{J_{e,x}Bu_{e,z}} = m_e\nu_{eff}\overline{\Gamma_{e,z}u_{e,z}}$. Reconstructing it and using equation (7), we have

$$\frac{|\tilde{J}_z|^2}{|\tilde{J}_x|^2} = \frac{\omega_{ce}^2}{\omega^2 + \nu_{eff}^2}. \tag{9}$$

Figure 4(c) shows a good proportional relationship between the ratio of z- to x-direction Ohmic heating and $\omega_{ce}^2/(\omega^2 + \nu_{eff}^2)$ up to 50 G. Recall that the Ohmic heating along the electric field change little with the magnetic field, the Ohmic heating induced by the Hall current in the $\boldsymbol{E} \times \boldsymbol{B}$ direction, which becomes the dominant heating component as the magnetic field increases, can be well approximated from the unmagnetized CCPs.

Figure 5 shows the time-averaged electron energy distribution functions (EEDFs) at magnetic fields of 0 and 50 G. A transition from bi-Maxwellian type to Druyvesteyn-like type is observed as applying a transverse magnetic field. At a low pressure of 10 mTorr, without the magnetic field, the energetic electrons entering the sheath are effectively heated through collisionless heating, while the low energy electrons in the bulk gain energy through Ohmic heating, resulting in a bi-Maxwellian distribution. With a transverse magnetic field, the mean free path of electrons is reduced, the collision frequency is improved, resulting in a suppression of the nonlocal electron motion which causes the EEDF grouping.

In summary, we have studied the enhancement of Ohmic heating in a magnetized CCP based on PIC simulations and a moment analysis of the Boltzmann equation, which self-consistently considers all the electron power absorption mechanisms and provides a comprehensive understanding of this complex phenomenon. We demonstrate that the enhanced Ohmic heating is induced by the Hall current in the $\boldsymbol{E} \times \boldsymbol{B}$ direction, which plays a major role as the magnetic field increases. The spatio-temporal dynamics of Ohmic heating in this direction is well described by the analytical formula of Ohmic heating with the Hall current. The ratio of Ohmic heating in different directions can be well approximated from the electron gyration, the voltage, and the collision frequencies, implying that the electron heating of a magnetized CCP discharge can be estimated from the unmagnetized CCPs.

Acknowledgments

This work was supported by the National Science Foundation awards #1700785, #1724941, and #1917577.

ORCID iDs

Bocong Zheng https://orcid.org/0000-0002-6052-3693

References

[1] Godyak V A and Piejak R B 1990 Abnormally low electron energy and heating-mode transition in a low-pressure argon rf discharge at 13.56 mhz *Phys. Rev. Lett.* **65** 996–9
[2] Godyak V A 1986 *Soviet Radio Frequency Discharge Research* (Falls Church, VA: Delphic Associates)
[3] Turner M M 1995 Pressure heating of electrons in capacitively coupled rf discharges *Phys. Rev. Lett.* **75** 1312–5
[4] Gozadinos G, Turner M M and Vender D 2001 Collisionless electron heating by capacitive rf sheaths *Phys. Rev. Lett.* **87** 135004
[5] Lafleur T, Chabert P, Turner M M and Booth J P 2014 Equivalence of the hard-wall and kinetic-fluid models of collisionless electron heating in capacitively coupled discharges *Plasma Sources Sci. Technol.* **23** 015016
[6] Turner M M, Hutchinson D A W, Doyle R A and Hopkins M B 1996 Heating mode transition induced by a magnetic field in a capacitive rf discharge *Phys. Rev. Lett.* **76** 2069–72
[7] You S J, Chung C W, Bai K H and Chang H Y 2002 Power dissipation mode transition by a magnetic field *Appl. Phys. Lett.* **81** 2529–31
[8] You S J, Kim S S and Chang H Y 2004 Low energy electron cooling induced by a magnetic field in high pressure capacitive radio frequency discharges *Appl. Phys. Lett.* **85** 4872–4
[9] You S J, Park G Y, Kwon J H, Kim J H, Chang H Y, Lee J K, Seong D J and Shin Y H 2010 Evolution of electron temperature in low pressure magnetized capacitive plasma *Appl. Phys. Lett.* **96** 101504
[10] Kushner M J 2003 Modeling of magnetically enhanced capacitively coupled plasma sources: Ar discharges *J. Appl. Phys.* **94** 1436–47
[11] Yang S, Zhang Y, Wang H-Y, Wang S and Jiang W 2017 Electrical asymmetry effects in magnetized capacitively coupled plasmas in argon *Plasma Sources Sci. Technol.* **26** 065011
[12] Surendra M and Dalvie M 1993 Moment analysis of rf parallel-plate-discharge simulations using the particle-in-cell with Monte Carlo collisions technique *Phys. Rev.* E **48** 3914–24
[13] Lafleur T, Chabert P and Booth J P 2014 Electron heating in capacitively coupled plasmas revisited *Plasma Sources Sci. Technol.* **23** 035010
[14] Schulze J, Donkó Z, Lafleur T, Wilczek S and Brinkmann R P 2018 Spatio-temporal analysis of the electron power absorption in electropositive capacitive rf plasmas based on moments of the Boltzmann equation *Plasma Sources Sci. Technol.* **27** 055010
[15] Surendra M, Graves D B and Jellum G M 1990 Self-consistent model of a direct-current glow discharge: treatment of fast electrons *Phys. Rev.* A **41** 1112–25
[16] Turner M M, Derzsi A, Donkó Z, Eremin D, Kelly S J, Lafleur T and Mussenbrock T 2013 Simulation benchmarks for low-pressure plasmas: capacitive discharges *Phys. Plasmas* **20** 013507
[17] Hutchinson D, Turner M, Doyle R and Hopkins M 1995 The effects of a small transverse magnetic field upon a capacitively coupled rf discharge *IEEE Trans. Plasma Sci.* **23** 636–43
[18] Lieberman M A and Lichtenberg A J 2005 *Principles of plasma discharges and materials processing* (New Jersey: Wiley)
[19] Chabert P and Braithwaite N 2011 *Physics of Radio-Frequency Plasmas* (New York: Cambridge University Press)
[20] Lafleur T, Chabert P, Turner M M and Booth J P 2013 'Anomalous' collisionality in low-pressure plasmas *Phys. Plasmas* **20** 124503